Multiplicity Dependence of the D_s^+/D^+ Yield Ratio, and Searches for D_s^{*+} and $D_{s1}(2460)^+$ in LHCb PbPb Collisions

Author: Manel Bosch Mesquida
Facultat de Física, Universitat de Barcelona, Diagonal 645, 08028 Barcelona, Spain.

Advisor: Ricardo Vázquez Gómez

Abstract: The multiplicity dependence of both the D_s^+/D^+ yield ratio and the prompt to non-prompt production fractions of the D^+ and D_s^+ mesons are studied in PbPb collision data at a center-of-mass energy of $\sqrt{s} = 5.02$ TeV. The data sample corresponds to an integrated luminosity of 230 μb^{-1} collected with the LHCb detector. An enhanced D_s^+ to D^+ production is observed with increasing multiplicity, compatible with the *strangeness enhancement* signature. Additionally, as multiplicity increases, the prompt to non-prompt D_s^+ production fraction manifests an increasing tendency, while the prompt to non-prompt D^+ production fraction exhibits a non-monotonic behavior. Furthermore, searches for the D_s^{*+} and $D_{s1}(2460)^+$ states are performed, both in the $D_s^+\gamma$ decay channel, but no evidence for the latter is found.
Keywords: Particle Detection, Charmed Mesons, Charmed Strange Mesons, Quark Gluon Plasma, and *Strangeness enhancement*.
SDGs: Quality Education, Clean and Sustainable Energy, and Climate Action.

I. INTRODUCTION

At low energies, particle interactions are governed by properties such as the *color confinement*, which states that unbounded quarks cannot exist. This environment, where such properties are expected, is commonly referred to as Cold Nuclear Matter (CNM). However, at extremely high energies and densities, a new state of matter is observed in which hadrons melt into their quark and gluon constituents, no longer obeying the *color confinement*, and allowing quarks to exist unbounded. This state is known as Quark Gluon Plasma (QGP), and since its life-time is on the order of 10 ys, it cannot be directly detected. Instead, its presence can only be inferred through certain signatures. One of these is the *strangeness enhancement*, which refers to the phenomenon wherein the production of strange quark-antiquark pairs is significantly enhanced under deconfining conditions (i.e, when a QGP is formed). As a result, when hadronization occurs, the formation of hadrons containing strange quarks becomes more likely, leading to an enhanced production of strange hadrons relative to non-strange ones, compared to the observed in a CNM environment.
Thus, PbPb collisions, and heavy-ion collisions in general, offer an interesting scenario for exploring particle formation mechanisms and studying how particles interact in high-energy and high-density environments. In these collisions, a QGP is often produced, and it can lead to different phenomena from those typically observed in a CNM environment.

In this work, the D_s^+/D^+ yield ratio and the prompt to non-prompt production fractions of both D^+ and D_s^+ mesons are studied as a function of multiplicity, to infer on the formation of a QGP via the *strangeness enhancement* signature. Unless stated otherwise, charge conjugation is implied throughout this work. Furthermore, when D^+ is referred to, it means the lightest charmed meson, with spin-parity quantum numbers $J^P = 0^-$, while D_s^+ refers to the lightest charmed strange meson, also with $J^P = 0^-$ spin-parity.

Additionally, PbPb collisions provide an interesting scenario where to study the nature of particles.
In recent years, some new resonances have been observed that do not fit into the framework of conventional hadrons, such as the $D_{s1}(2460)^+$ state first observed in 2003 [1]. It was proposed to be the expected charmed strange meson with quantum numbers $J^P = 1^+$ in the Quark Model. However, it was lighter than predicted, and some of its expected decay channels were not found. A hypothesis that could explain the above properties is that it is not a charmed strange meson, but a tetraquark — a state consisting of four bounded quarks.

Thus, this work also aims to achieve a better understanding of the nature of the $D_{s1}(2460)^+$ state.
To accomplish this, is intended to study the multiplicity dependence of the $\sigma(\text{PbPb} \to D_{s1}(2460)^+X)/\sigma(\text{PbPb} \to D_s^{*+}X)$ ratio, where X refers to any other PbPb collision product. As the D_s^{*+} state is the charmed strange meson with $J^P = 1^-$ spin-parity, an evidence for the $D_{s1}(2460)^+$ state not being a charmed strange meson would be finding that ratio not remaining constant. The same strategy was employed in an analysis of the nature of the $\chi_{c1}(3872)$ hadron [3].

II. DETECTOR AND DATASET

The analysis presented in this work is based on LHCb PbPb collision data collected in 2018, at a center-of-mass

energy of $\sqrt{s} = 5.02$ TeV, which correspond to an integrated luminosity of 230 μb^{-1}.
The LHCb detector is a forward spectrometer that covers the pseudorapidity range $2 \leq \eta \leq 5$, optimized for the study of heavy flavor hadrons. It is composed of a calorimetric system located downstream of the tracking stations, which includes a scintillating pad detector (SPD) and a pre-shower detector (PS) for particle identification, an electromagnetic calorimeter (ECAL) composed of lead scintillator tiles with fine granularity, and a hadronic calorimeter (HCAL) using iron scintillator modules. The tracking system consists of a high-precision silicon-strip vertex detector called VELO (VErtex LOcator) surrounding the collision region, a large-area silicon-strip detector located upstream of a dipole magnet with a bending power of about 4 T · m, and three stations of silicon-strip detectors and straw drift tubes placed downstream of the magnet.

III. NATURE OF THE $D_{s1}(2460)^+$ STATE

To achieve a better understanding of the nature of the $D_{s1}(2460)^+$ state, it is intended to study the multiplicity dependence of the $\sigma(\text{PbPb} \to D_{s1}(2460)^+X)/\sigma(\text{PbPb} \to D_s^{*+}X)$ ratio. For this purpose, the D_s^{*+} and $D_{s1}(2460)^+$ states have been reconstructed, focusing on the $D_s^+\gamma$ decay channel which has a branching ratio of $93.6 \pm 0.4\%$ and $18 \pm 4\%$, respectively [4]. As a first step, the D_s^+ meson mass distribution has been reconstructed.

A. The D_s^+ Meson Signal

The reconstruction of the D_s^+ meson mass distribution has been focused in the $D_s^+ \to \phi\pi^+$ decay channel, which has a branching ratio of $2.21 \pm 0.06\%$ [4]. The $\phi\pi^+$ state has been reconstructed with the ϕ meson decaying to the K^+K^- state, as it provides the best signal over background significance.
With regard to the selection of the D_s^+ mesons candidates, it has been used the criteria described in an analysis of the production of D^+ and D_s^+ mesons in LHCb pPb collisions [2], focused on reducing the background. The candidates are required to have a good vertex and track fit quality, as well as a reliable particle identification. To isolate the $\phi\pi^+$ component of the reconstructed $K^+K^-\pi^+$ state, the invariant mass of the K^+K^- state has been required to be within a tight window centered around the ϕ meson mass, whose value is taken from the PDG [4]. Thus, from now on, when $K^+K^-\pi^+$ is referred to, it is implicit that the K^+K^- pair comes from a ϕ meson. On the other hand, due to limited statistics at high D_s^+ meson transverse momentum, additional cuts have been applied, by imposing transverse momentum and rapidity constraints within certain ranges. It is also ensured that the particles had a kinematic pseudorapidity consistent with the detection range of the LHCb detector. Additionally, the tracks of the three daughters are required to not originate from the primary vertex, whereas the D_s^+ candidates are required to do so. For the last, it is also important to differentiate between prompt and non-prompt D_s^+ mesons, as the non-prompt ones are produced when the QGP has already cooled. Unless stated otherwise, all the analyses have been done using only promptly produced candidates. The prompt D_s^+ candidates have been selected by requiring their flight-distance from the primary vertex to be below a certain threshold.
This offline selection criteria yields the invariant mass distribution of the $K^+K^-\pi^+$ state plotted in figure 1.

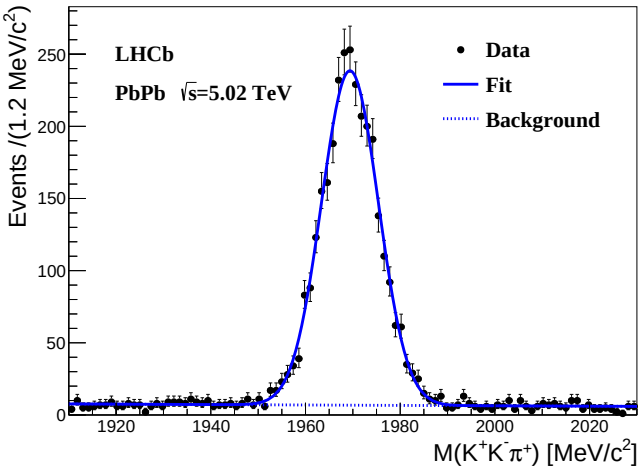

FIG. 1: Distribution of the invariant mass $M(K^+K^-\pi^+)$ for events satisfying the cuts described in the text. The points correspond to the LHCb data, while the overlaid curve represents the results from a fit of the data to a Gaussian signal function plus an exponential background function.

From a binned maximum likelihood fit of the $M(K^+K^-\pi^+)$ distribution to a Gaussian signal shape and an exponential background function, in which Gaussian and exponential parameters are allowed to float, a yield of 2906 ± 57 events has been obtained in the peak.

Thus, the existence of a peak in the $K^+K^-\pi^+$ mass spectrum compatible with the D_s^+ meson is confirmed, as the obtained Gaussian mean is consistent with the D_s^+ meson mass value proportioned by the PDG [4]. The given errors are due to statistics only.

B. The D_s^{*+} Meson Signal

Once the D_s^+ meson mass distribution has been reconstructed, the analysis has been focused on the D_s^{*+} state, via the $D_s^{*+} \to D_s^+\gamma$ decay channel. Its reconstruction has been carried out by only selecting photon candidates with a high confidence level of being a photon, and requiring them to be emitted close to the flight

direction of the D_s^+ meson. Additionally, all the D_s^+ mesons candidates are required to have a mass equal to the world-measured, $m_{PDG}(D_s^+)$. To do it, the analysis has been performed with a variable which has been called the constrained mass, defined as $M(K^+K^-\pi^+\gamma) - M(K^+K^-\pi^+) + m_{PDG}(D_s^+)$. For simplicity, throughout this work it will referred just as $M(K^+K^-\pi^+\gamma)$.
Furthermore, the search has been centered just on the vicinity of the expected D_s^{*+} meson mass peak. The distribution of the constrained invariant mass $M(K^+K^-\pi^+\gamma)$ is plotted in figure 2.

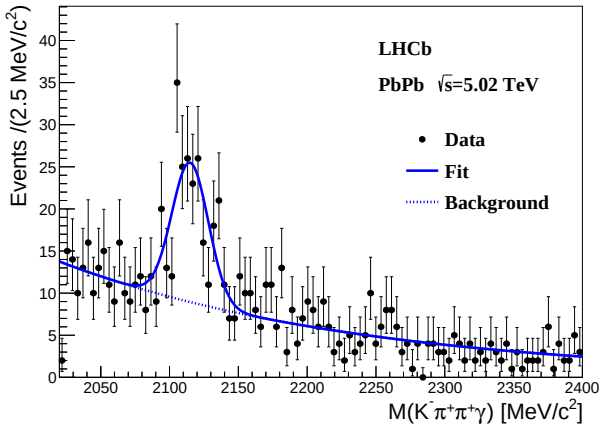

FIG. 2: Distribution of the constrained invariant mass $M(K^+K^-\pi^+\gamma)$ for events satisfying the cuts described in the text. The points correspond to the LHCb data, while the overlaid curve represents the results from a fit of the data to a Gaussian signal function plus an exponential background function.

The data has been fitted to a model performed as a Gaussian signal function plus an exponential background function. The Gaussian mean and width are allowed to float, as well as the exponential slope. A binned maximum likelihood fit of the data to the model has determined the yield in the peak to be 148±20 events. Once more, errors are only due to statistics.

C. Searches for the $D_{s1}(2460)^+$ State

To reconstruct the $D_{s1}(2460)^+$ state in the $D_s^+\gamma$ decay channel, the same strategy as for the D_s^{*+} meson has been followed, and no additional cuts have been applied beyond the already described. But the study of the mass spectrum has been centered in a window near the expected $D_{s1}(2460)^+$ state mass peak.

The distribution of the constrained invariant mass $M(K^+K^-\pi^+\gamma)$ near the expected $D_{s1}(2460)^+$ state mass peak is plotted in figure 3.

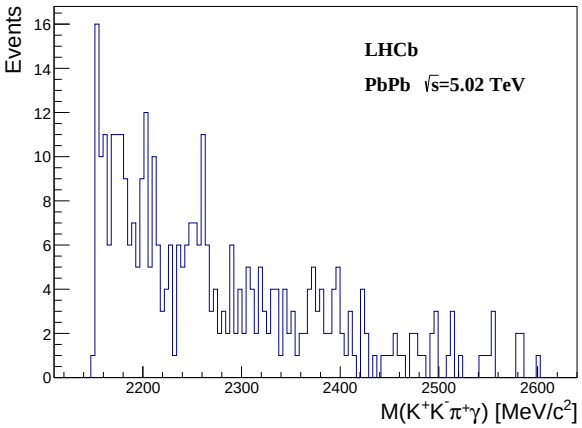

FIG. 3: Constrained mass distribution $M(K^+K^-\pi^+\gamma)$ in the 2460 MeV/c^2 vicinity, where the $D_{s1}(2460)^+$ state mass peak would be expected. The histogram yields correspond to the LHCb data.

As can be seen in figure 3, it is not observed any structure in the spectrum near 2460 MeV/c^2, where a signal from the $D_{s1}(2460)^+$ state decay would be expected. The most likely explanation is that there is not enough data to reconstruct the $D_{s1}(2460)^+$ state. Although unlikely, the existence of dissociation mechanisms operating at such high energies, as the already reported J/ψ suppression [5], cannot be ruled out.

Since no evidence for the $D_{s1}(2460)^+$ state has been found, its nature cannot be studied.

IV. MULTIPLICITY DEPENDENCE OF PROMPT D_s^+ AND D^+ MESONS PRODUCTION

The multiplicity dependence of both the D_s^+/D^+ yield ratio and the prompt to non-prompt D_s^+ and D^+ mesons production fractions could provide insights into the presence of a QGP and help to understand the processes occurring within it.
To carry out this work, first has been searched for the D^+ meson by reconstructing the $K^-\pi^+\pi^+$ state. That decay channel has a branching ratio of $9.8 \pm 0.16\%$ [4].

A. The D^+ Meson Signal

To reconstruct the D^+ meson in the $D^+ \to K^-\pi^+\pi^+$ decay channel, the same selection criteria as for the reconstruction of the D_s^+ meson has been considered, but with a different flight-distance threshold value to discern between prompt and non-prompt D^+ meson candidates.

The mass distribution $M(K^-\pi^+\pi^+)$ obtained after

applying these cuts, is plotted in figure 4.

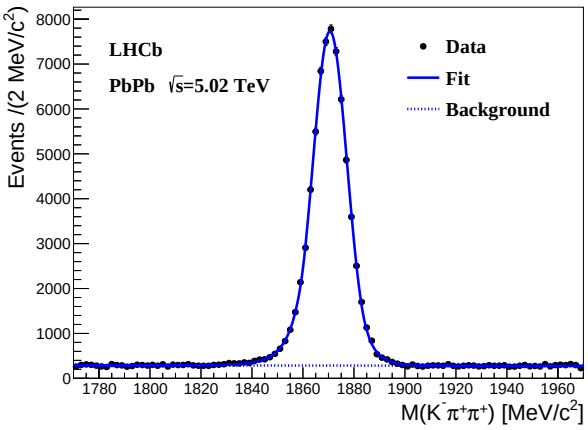

FIG. 4: Distribution of the invariant mass $M(K^-\pi^+\pi^+)$ for events satisfying the cuts described in the text. The points represents the LHCb data while the overlaid curve correspond to the results from a fit of the data to a Double Sided Crystal Ball signal function plus an exponential background function.

The fit model is a Double Sided Crystal Ball function (DSCB) plus an exponential background function. A Double Sided Crystal Ball function consists of a Gaussian core portion and two sided power-law low-end tails, below certain thresholds.
The DSCB and exponential parameters are allowed to float. From a binned maximum likelihood fit of the data to the model, a yield of 64930 ± 277 events has been obtained in the peak.

Thus, the existence of a peak in the $K^-\pi^+\pi^+$ mass spectrum compatible with the D^+ meson is confirmed. The DSCB mean is consistent with the D^+ meson mass value proportioned by the PDG [4]. The given errors are due to statistics only.

B. The D^+ and D_s^+ Prompt to Non-Prompt Production Fractions

The prompt to non-prompt production fractions of both the D_s^+ and D^+ mesons, which will be referred as f_{prompt}, have been studied depending on the multiplicity, which refers to the number of tracks produced at the primary vertex. The multiplicities are determined with the "nVeloTracks" variable (i.e the tracks reconstructed in the VELO).
Once the prompt D_s^+ and D^+ mesons mass distributions have been reconstructed, the same selection criteria for the non-prompt have been used, changing only that candidates must have a larger flight-distance than the threshold value used to determine the prompt ones.
The *sPlot* technique [6] has been used with the non-prompt D^+ meson yields in order to unfold the signal and background distributions, with the invariant mass as control variable. Using the weights provided by *sPlot*, the variable "nVeloTracks" has been weighted to isolate the signal distribution, and then its cumulative distribution has been extracted.
Thus, using the cumulative distribution, the "nVeloTracks" bins are selected based on the criterion of being equally populated with non-prompt D^+ meson yields.
On the other hand, the prompt D^+ meson yields have been determined by fitting its mass distribution with only candidates produced in events with a number of "nVeloTracks" within the range of the selected bins.
The same strategy has been followed for the D_s^+ meson. Finally, for both mesons and for each bin, the fraction f_{prompt} has been calculated. The result is shown in figure 5.

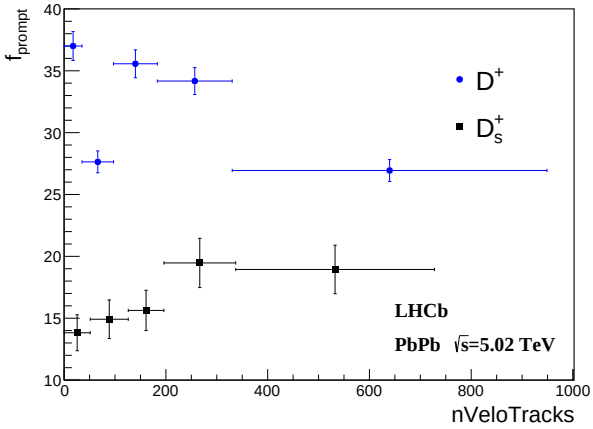

FIG. 5: Fraction f_{prompt}, of promptly produced D^+ and D_s^+ mesons to non-prompt ones, as a function of the number of tracks reconstructed in the VELO. The vertical error bars correspond to the statistical uncertainties provided by the fits, while horizontal ones indicate the bin widths.

For the D_s^+ meson, f_{prompt} is found to increase with multiplicity, thus can be inferred that the prompt formation mechanisms for D_s^+ mesons are more effective in high-multiplicity environments, which is consistent with the *strangeness enhancement* in a QGP environment.
And for the D^+ meson, f_{prompt} exhibits a non-monotonic behavior as multiplicity increases.

C. The D_s^+/D^+ Yield Ratio

For the purpose of studying the D_s^+/D^+ yield ratio as a function of multiplicity, the same procedure as the explained in the previous section has been followed. In this case, the *sPlot* technique has been used with the D_s^+ meson yields, also with the invariant mass as control variable. The "nVeloTracks" bins are selected based on the criterion of being equally populated with D_s^+ mesons, and the D^+ meson yields are determined

by fitting its mass distribution with only candidates produced in events with a number of "nVeloTracks" within the range of the already selected bins.
Finally, for each bin, the fraction D_s^+/D^+ has been calculated. The result in shown in figure 6.

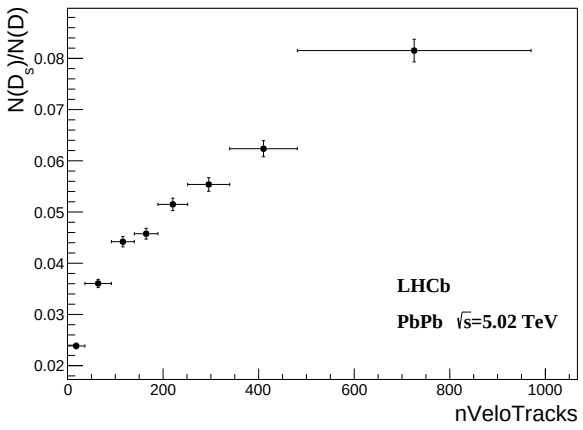

FIG. 6: The D_s^+/D^+ yield ratio as a function of the tracks reconstructed in the VELO. The vertical error bars correspond to the statistical uncertainties provided by the fits, while horizontal ones indicate the bin widths.

The D_s^+/D^+ yield ratio is found to increase with multiplicity. And as high-multiplicity events are directly related to high-energy and high-density environments, can be inferred that the observed behavior is consistent with the *strangeness enhancement*. Furthermore, it also suggest that meson dissociation mechanisms do not dominate over the *strangeness enhancement*, where the strong force that binds quarks into hadrons, can weaken or become ineffective over short timescales.

V. CONCLUSIONS AND FURTHER WORK

A. Conclusions

In summary, data from the LHCb detector have enabled the reconstruction of the D_s^+, D_s^{*+} and D^+ mesons, but not the $D_{s1}(2460)^+$ state. As mentioned, the most likely explanation for the $D_{s1}(2460)^+$ state not being found is an insufficient amount of data.
On the other hand, the D_s^+/D^+ yield ratio is found to increase with multiplicity, indicating an enhanced production of D_s^+ relative to D^+ mesons, consistent with the *strangeness enhancement*.
Furthermore, an enhanced production of prompt relative to non-prompt D_s^+ mesons is observed as multiplicity increases. That tendency is also compatible with the *strangeness enhancement*, as it manifests an enhanced production of D_s^+ mesons in the nearly stages after the collision (i.e in the hypothetical QGP), relative to the non-early produced.

B. Further Work

To obtain more accurate results, the correction efficiencies must be taken into account. These might be different for both D_s^+ and D^+ mesons, and depend on multiplicity, meaning that they could significantly influence the tendency of the D_s^+/D^+ ratio. In the current work, the ratio of efficiencies has been considered to be one.
Furthermore, a larger amount of data would be necessary to obtain more precise results and to compare them with Monte Carlo simulations. Moreover, it would likely enable the reconstruction of the $D_{s1}(2460)^+$ state, as well as investigate its nature using the strategy proposed in this work.
Finally, a study of systematic uncertainties should be conducted, and a more accurate technique to distinguish prompt from non-prompt production is also needed.

Acknowledgments

I'd like to express my profound gratitude to my advisor, Ricardo Vázquez Gómez, for his invaluable guidance, and the perspective about topics he provided me, as well as my family for their unconditional support during all these years. I also thanks people working on CERN for the excellent performance of LHCb.

[1] The CLEO Collaboration. Observation of a Narrow Resonance of Mass 2.46 GeV/c^2 Decaying to $D_s^{*+}\pi^0$ and Confirmation of the $D_{sJ}^*(2317)$ State. Phys. Rev. D, 68, 032002 (2003).
[2] The LHCb Collaboration. Measurement of prompt D^+ and D_s^+ production in pPb collisions at $\sqrt{s_{NN}} = 5.02$ TeV at LHCb. Journal of High Energy Physics, 2024, 070 (2024).
[3] The LHCb Collaboration. Observation of multiplicity-dependent prompt $\chi_{c1}(2872)$ and $\psi(2S)$ production in pp collisions. Phys. Rev. Lett., 126, 092001 (2021).
[4] S. Navas *et al.* (Particle Data Group). Phys. Rev. D, 110, 083501 (2024).
[5] The NA50 Collaboration. A new measurement of J/ψ suppression in Pb-Pb collisions at 158 GeV per nucleon. The European Physical Journal C, 39, 335–345 (2005)
[6] M. Pivk and F. R. Le Diberder. A statistical tool to unfold data distributions. Nucl. Instrum. Meth, 555, 356–369 (2005).

Dependència en la Multiplicitat del Quocient d'Esdeveniments D_s^+/D^+, i Recerca dels Estats D_s^{*+} i $D_{s1}(2460)^+$ en Col·lisions Pb-Pb al LHCb.

Author: Manel Bosch Mesquida
Facultat de Física, Universitat de Barcelona, Diagonal 645, 08028 Barcelona, Spain.

Advisor: Ricardo Vázquez Gómez

Resum: En aquest treball s'ha estudiat la dependència en la multiplicitat del quocient d'esdeveniments D_s^+/D^+, així com de les fraccions dels mesons D^+ i D_s^+ inmediatament produïts en els primers estadis després de la col·lisió. Tot això s'ha fet usant les dades de col·lisions Pb-Pb registrades en el LHCb, amb una energia del centre de masses de $\sqrt{s}$ =5.02 TeV, i corresponents a una lluminositat integrada de 230 μb^{-1}. S'ha observat un increment en la producció de mesons D_s^+ en relació als mesons D^+, a mesura que augmenta la multiplicitat, cosa compatible amb la signatura de *strangeness enhancement*. A més, pels mesons D_s^+ també s'ha mesurat un increment en la fracció dels produïts de forma immediata. I, per altra banda, un comportament no monòton d'aquesta mateixa fracció pels mesons D^+. Finalment, també s'ha fet una recerca dels estats D_s^{*+} i $D_{s1}(2460)^+$, ambdós en el canal de desintegració $D_s^+\gamma$, tot i que no s'ha trobat cap evidència per aquest últim.

Paraules clau: Detecció de Partícules, Mesons Encantats, Mesons Encantats Estranys, Plasma de Quarks i Gluons, i *Increment de l'Estranyesa.*

ODSs: Aquest TFG està relacionat amb els Objectius de Desenvolupament Sostenible (SDGs)

Objectius de Desenvolupament Sostenible (ODSs o SDGs)

1. Fi de les desigualtats		10. Reducció de les desigualtats	
2. Fam zero		11. Ciutats i comunitats sostenibles	
3. Salut i benestar		12. Consum i producció responsables	
4. Educació de qualitat	X	13. Acció climàtica	X
5. Igualtat de gènere		14. Vida submarina	
6. Aigua neta i sanejament		15. Vida terrestre	
7. Energia neta i sostenible	X	16. Pau, justícia i institucions sòlides	
8. Treball digne i creixement econòmic		17. Aliança pels objectius	
9. Indústria, innovació, infraestructures			